APL Photonics

Line-of-sight and non-line-of-sight links for dispersive terahertz wireless networks

Cite as: APL Photonics **6**, 041304 (2021); https://doi.org/10.1063/5.0039262
Submitted: 01 December 2020 . Accepted: 14 March 2021 . Published Online: 27 April 2021

Yasaman Ghasempour, Yasith Amarasinghe, Chia-Yi Yeh, Edward Knightly, and Daniel M. Mittleman

Line-of-sight and non-line-of-sight links for dispersive terahertz wireless networks

Cite as: APL Photon. 6, 041304 (2021); doi: 10.1063/5.0039262
Submitted: 1 December 2020 • Accepted: 14 March 2021 •
Published Online: 27 April 2021

Yasaman Ghasempour,[1] Yasith Amarasinghe,[2] Chia-Yi Yeh,[1] Edward Knightly,[1] and Daniel M. Mittleman[2,a)]

AFFILIATIONS

[1] Department of Electrical and Computer Engineering, Rice University, 6100 Main St., Houston, Texas 77005, USA
[2] School of Engineering, Brown University, 184 Hope Street, Providence, Rhode Island 02912, USA

[a)] **Author to whom correspondence should be addressed:** daniel_mittleman@brown.edu

ABSTRACT

Despite the rapidly growing interest in exploiting millimeter and terahertz waves for wireless data transfer, the role of reflected non-line-of-sight (NLOS) paths in wireless networking is one of the least explored questions. In this paper, we investigate the idea of harnessing these specular NLOS paths for communication in directional networks at frequencies above 100 GHz. We explore several illustrative transmitter architectures, namely, a conventional substrate-lens dipole antenna and a leaky-wave antenna. We investigate how these high-gain directional antennas offer both new challenges and new opportunities for exploiting NLOS paths. Our results demonstrate the sensitivity to antenna alignment, power spectrum variations, and the disparity in supported bandwidth of various line-of-sight (LOS) and reflected path configurations. We show that NLOS paths can, under certain circumstances, offer even higher data rates than the conventional LOS path. This result illustrates the unique opportunities that distinguish THz wireless systems from those that operate at lower frequencies.

The role of reflected paths has been extensively studied in microwave systems for many years.[1–6] In such systems, non-line-of-sight (NLOS) paths are conventionally known to affect channel fading,[1,2] inter-user interference,[3,4] or offer spatial diversity for multiplexing via increasing the channel's degrees of freedom.[5,6] At these lower frequencies, there is typically no distinction drawn between a specular reflection and diffuse scattering, since broadcasts are usually quasi-omnidirectional, not in the form of directional beams. At frequencies in the 100–500 GHz range, the situation is quite different, more reminiscent of the realm of optics. Since most envisioned applications in this range of the spectrum, including sensing, communications, and imaging, will likely rely on highly directional transmissions (i.e., beams), the role of NLOS paths is quite different. One important example emerges from the idea of wireless communication links. In a directional wireless network, the line-of-sight (LOS) propagation, usually envisioned to be the preferred communication channel, is susceptible to being completely blocked due to obstacles, e.g., people walking through the beam path.[7–11] In such a situation, one can envision exploiting a previously characterized NLOS path in order to maintain connectivity, a fundamental need for any wireless network. So far, despite the rapidly growing interest in exploiting millimeter and terahertz waves for wireless data transfer, there has been little attention devoted to the understanding and use of NLOS paths in this spectral range,[12–17] as the majority of work has focused on LOS paths.[18–20]

In this paper, we investigate the idea of harnessing the specular NLOS paths for communication at frequencies above 100 GHz, in several illustrative transmitter and receiver architectures. Here, we distinguish between specular NLOS paths, in which the signal is reflected from a surface as if it were a mirror,[21] and non-specular NLOS paths in which the reflection is from a rough surface and produces a diffuse (and therefore no longer directional) beam.[16] As noted above, this distinction is not present in conventional low-frequency systems, since there is no directional incident beam that can form a coherent reflected beam in a particular direction. Thus, these considerations are unique to millimeter-wave and terahertz links, offering both new challenges and new opportunities for system design. We note that, at lower frequencies below ~6 GHz, the link budget of NLOS paths has been studied extensively, suggesting lower signal-to-noise ratio (SNR) due to extra propagation distance compared to the LOS path as well as additional dielectric and scattering losses as a result of interaction with reflecting surfaces. In

the range of interest here (above 100 GHz), such losses are expected to increase even further (relative to the LOS path), ultimately limiting their use for data communication. However, there has so far been little quantitative evaluation of this idea, so the understanding of how to exploit NLOS paths in THz networks remains an open challenge.

Recently, there have been several studies of LOS and NLOS channel models in the THz regime. Researchers have incorporated molecular absorption into the path loss,[7] considered the reflection properties of typical indoor material in the 0.1–1 THz frequency range,[22,23] and begun to address the scattering behavior of rough surfaces in specular[24] and non-specular[25,26] directions. Such studies confirm that strong reflected-path NLOS signals can exist, especially in indoor environments, at frequencies up to 300 GHz;[27] however, they have so far stopped short of considering the challenges of data transfer over such links. In particular, one key factor that has not been studied is the implication of using high-gain directional antennas that are likely to be less sensitive to signals arriving from NLOS directions. With the use of high-gain antennas, the adaptation of both the transmitter and receiver beam directions to NLOS signals arriving from different directions is likely to be necessary in order to provide the highest link quality. Here, we consider this challenge in two interesting situations: (i) The transmitter and receiver are each equipped with a substrate-lens coupled dipole with a known antenna pattern that is a fairly narrow cone. This is representative of conventional high-gain antennas. (ii) A leaky-wave antenna is employed at

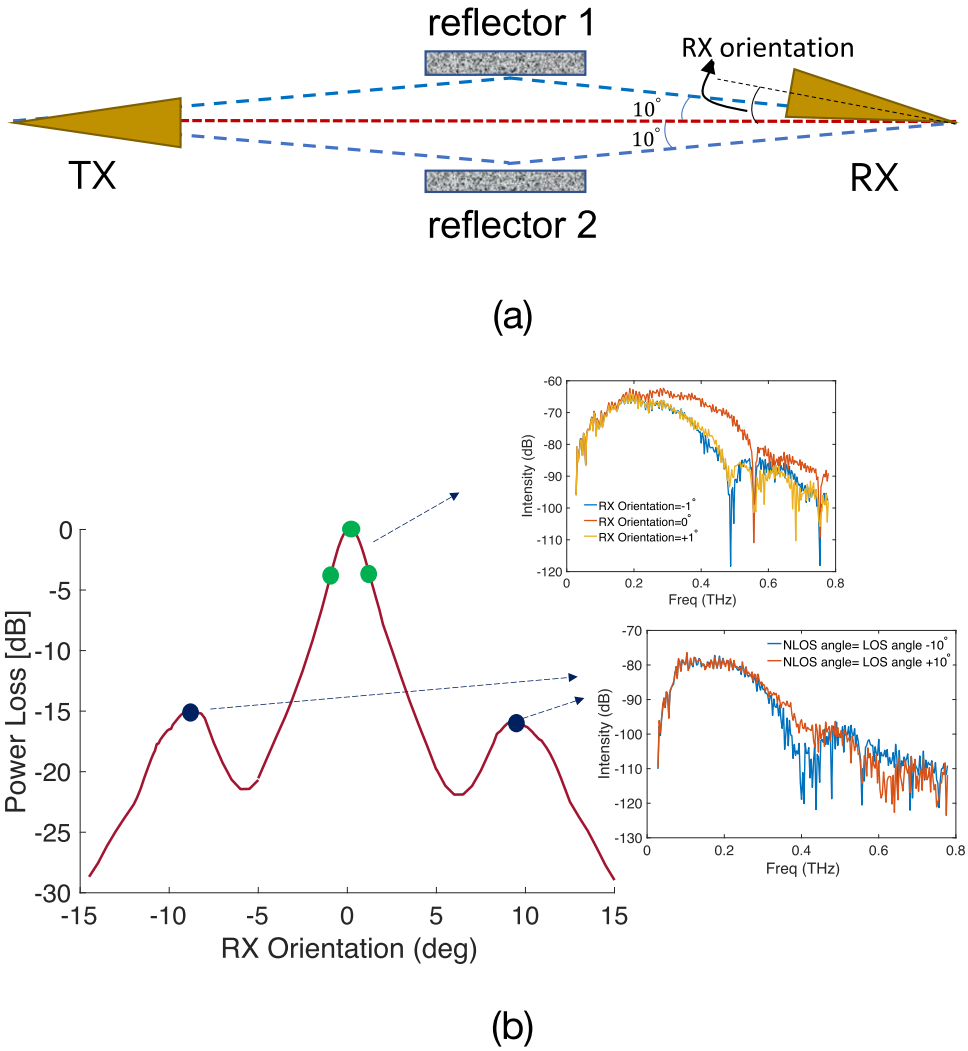

FIG. 1. (a) A schematic of the experiment consisting of two reflectors at 10° of the LOS path on either side. Depending on the RX orientation, a different path is captured by the substrate-lens coupled dipole antenna. (b) The power loss as a function of RX orientation when a substrate-lens coupled dipole antenna at the transmitter is emitting wideband THz pulses. Two reflectors are placed such that the geometric NLOS angle from the center of the reflector to the detector is 10° apart from the LOS angle (i.e., NLOS angle = LOS angle ±10°). The insets show the measured power spectrum for two cases: (i) when the RX is rotated by 1° on either side relative to the true LOS angle; (ii) when the RX is pointing to the middle of the reflectors creating the NLOS angles.

the transmitter or receiver so that the antenna radiation pattern is strongly frequency-dependent. Leaky-wave antennas are promising candidates for future THz wireless networks as they enable efficient frequency-controlled beam steering,[31] one-shot path discovery,[32,33] and multiplexing and demultiplexing of multiple users.[36] We show that a leaky-wave antenna at the transmitter creates a very different situation with some unique advantages.

First, we employ a substrate-lens coupled dipole antenna at the transmitter emitting wideband THz pulses, as is conventionally used for terahertz photoconductive antennas.[28] Here, the radiation pattern is determined by diffraction through the lens aperture and is only relatively weakly dependent on frequency.[29,30] We construct a test bed in which the transmitter (TX) is fixed and the receiver (RX) is held in rotatable mounts, with a TX-to-RX LOS distance of 80 cm. At two locations off of the direct LOS path between them, we place two reflectors such that the specular NLOS angle from the center of the reflector to the RX is 10° apart from the LOS angle (i.e., NLOS angle = LOS angle ± 10°). Since the half-power beamwidth of these conventional antennas is roughly 4°, we rotate the RX to emulate a wider beamwidth and capture different multipath components. Figure 1 depicts the power loss in dB as a function of RX orientation. Unsurprisingly, we observe that the received power is highly sensitive to the RX's orientation. Yet, the change in the spectral content of the received signal is independent of the rotation direction. In particular, lower frequency components are always more resilient against the RX orientation, since they produce a larger spot size at the receiver. As expected, the received power increases at rotation angles of ±10°, when a reflected path is captured. Furthermore, the spectrum for the reflected path is independent of the NLOS angle since all frequencies emit and distribute approximately uniformly in space.

As a contrast with the previous case, we next employ a leaky-wave antenna as the transmitter. This consists of a metal waveguide with an aperture opened on one side to permit radiation to "leak" out into free space if the guided mode and the free-space mode satisfy a phase-matching constraint on their parallel wave vector components. For the simplest architecture, a parallel-plate metal wave-guide with empty space between the plates, with the lowest-order transverse electric (TE_1) mode propagating in the waveguide, this phase-matching requirement imposes a constraint on the angle of propagation of the emitted radiation, for a given frequency f,

$$f(\phi) = \frac{c_0}{2b \sin\phi}, \tag{1}$$

where b is the plate separation (equal to 1 mm in our experiments), c_0 is the vacuum light velocity, and ϕ is the propagation angle of the free-space mode relative to the waveguide propagation axis. This relationship between the angle of emission and frequency makes this device a promising candidate for beam steering at frequencies above 0.1 THz by tuning the input frequency. Prior work has demonstrated the feasibility of modulated data transmission with leaky-wave antennas.[31]

The idea of adopting a leaky-wave antenna in multipath settings is illustrated schematically in Fig. 2. We excite the TE_1 mode of the waveguide with a broadband source such that different frequencies decompose and emerge at different angles from the waveguide, as a terahertz rainbow.[32–35] We place the RX (a substrate-lens-coupled antenna, as described above) at 45° relative to the waveguide axis, so that the LOS path corresponds to a frequency of 212 GHz, according to Eq. (1). We then mount an aluminum reflector on a rail that runs perpendicular to the TX-RX axis such that the face of the reflector is parallel to the LOS path. This allows us to create different NLOS configurations, by moving the reflector along the rail. For each reflector position, a portion of the emitted signal travels along the LOS path and a different portion *with spectrally distinct characteristics* reaches the RX via the NLOS path, by bouncing off the reflector (see Fig. 2). For each reflector position, we measure the signal with and without the reflector so that, by subtracting the two, we can remove the potential background LOS signal and isolate the NLOS path. We also rotate the receiver as in Fig. 1 to optimize for the integrated received power over time in the LOS/NLOS detection. We note that the spectral profile of the input THz source is not uniform causing various frequencies emitted by the leaky waveguide to be weighted in addition to the effects of Eq. (1). To focus specifically on the performance of the antenna, we measure and compensate for the spectrum of the THz source offline. Figure 3 illustrates both time-

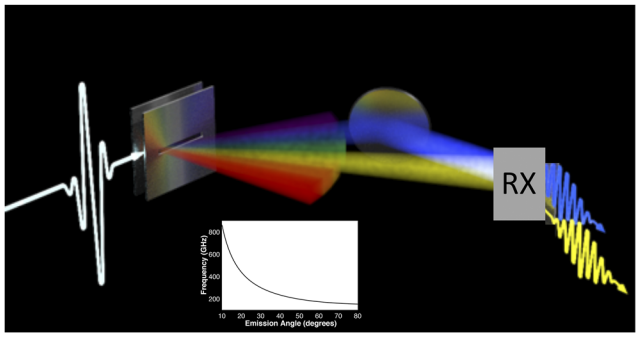

(a)

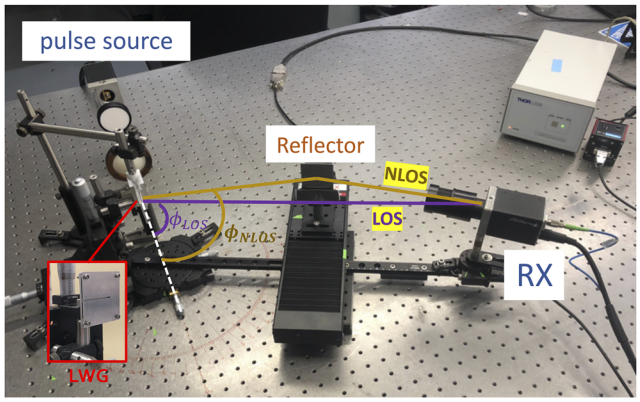

(b)

FIG. 2. (a) An illustration showing different frequencies (represented by "colors") emitting at different angles by a leaky waveguide excited by a broadband input signal. The plot shows the peak frequency (in GHz) that emits at each angle (in degrees). (b) Our experimental setup including a pulse source and detector, a custom-built leaky waveguide, and motorized rotation and translation stages to investigate different multipath configurations and RX orientations.

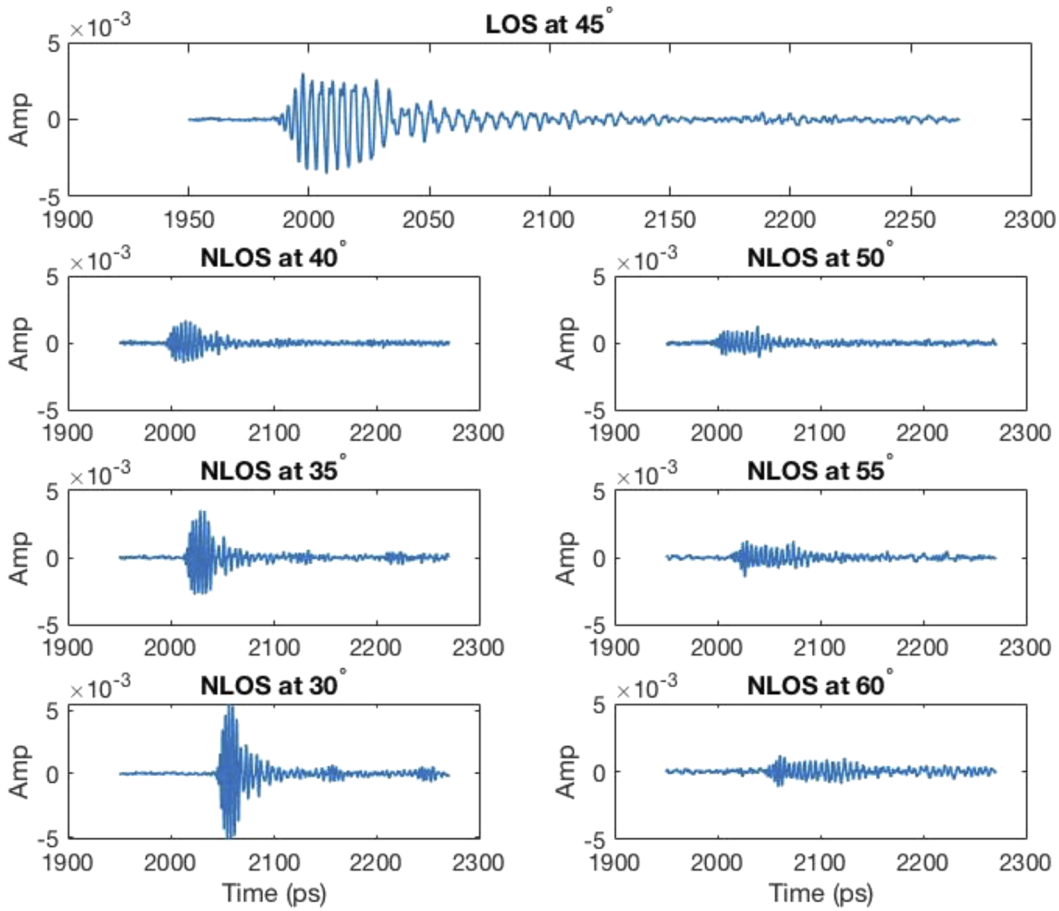

(a)

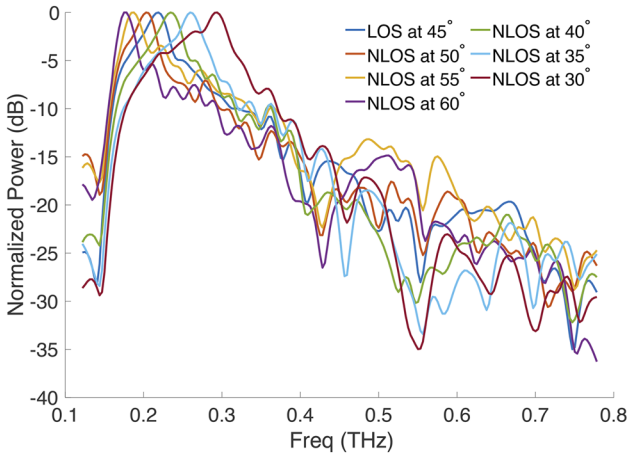

(b)

FIG. 3. The time-domain and frequency-domain signals for the LOS path, as well as for several different NLOS configurations with a LWA TX. With a larger NLOS angle, the spectral peak shifts to lower frequencies, while at smaller NLOS angles, it shifts to higher frequencies. The signals also broaden in the time domain for larger NLOS angles, but little or no broadening is observed for smaller NLOS angles.

domain and frequency-domain signals for the LOS path as well as for several different NLOS configurations. We see that at a larger NLOS angle, the spectral peak shifts to lower frequencies, while at smaller NLOS angles, it shifts to higher frequencies. These spectral shifts are consistent with the predictions of Eq. (1), since these signals were emitted from the TX waveguide at different angles, and therefore must contain different spectral content. Note that the antenna does not radiate well close to 0° and 90°; hence, the approximate angular range that could be effectively covered by a single leaky-wave antenna is roughly 10°–80°.[33] Furthermore, from Fig. 3, we observe that the signals also broaden in the time domain for larger NLOS angles, but little or no broadening is observed for smaller NLOS angles. This broadening is a consequence of the nonlinearity of the frequency–angle relationship shown in Eq. (1). For a fixed receiver aperture, the width of the received spectrum is determined by the angular dispersion of the emitted signal, which increases with decreasing frequency,[36] as discussed further below.

We next repeat the same setup as in Fig. 1 in which we create both a LOS angle of 45° and two NLOS angles at 35° and 55°. As before, we rotate the receiver and record the measured spectrum as a function of the receiver rotation angle. We then process the total received power at each RX orientation capturing different paths. To explore the relative properties of LOS and NLOS paths, we normalize the received power to the maximum power received across all configurations (achieved when the RX is perfectly oriented toward the LOS direction). Figure 4 summarizes these results. When the RX is oriented toward the NLOS path, the received power is comparable to the achievable power over the LOS path. We note that this is very different from the observation in Fig. 1 without a leaky-wave transmitter. The leaky waveguide acts as a directional antenna that steers different frequencies to different directions and hence provides a frequency-dependent directivity gain that boosts the NLOS link budget. Interestingly, the power loss (relative to the LOS path) is not symmetric for the two NLOS paths at 45° ± 10°. Furthermore, we observe that the spectral characteristics of the received signal depend on the path angle due to the spatial–spectral coupling. Finally, given a fixed RX aperture, misaligning the RX from the optimum LOS direction by 1° on either side impacts the measured spectrum differently. The underlying cause for all of these observations is embodied in Eq. (1): signals impinging on a different portion of the detector aperture carry different spectral content.

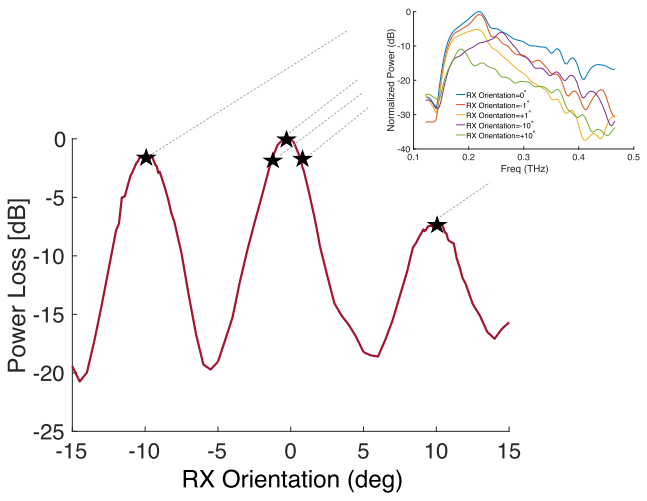

FIG. 4. Measured power as a function of receiver rotation angle in a three-path channel in which the LOS is at the angle of 45° and two NLOS paths exist at 35° and 55°. The inset shows the measured power spectrum when the RX is pointing directly to the LOS/NLOS directions and when it is misaligned from the LOS path by 1° on either side.

Multipath Characterization: Temporal vs Spectral Scheme. Distinguishing different components of a multipath wireless channel based on time of arrival (TOA) is one of the most common and well-known techniques. Here, by adopting a leaky waveguide at the transmitter, we also have a new opportunity to detect paths based on their spectral signatures. Recognizing that coherent detectors are significantly more challenging to build and operate, it is important to assess the costs and benefits of coherent systems that can offer reliable timing information against non-coherent schemes that rely solely on measuring the intensity at different frequencies. In designing a multi-path characterization scheme, one might need to consider the physics of the emitter. In particular, the nonlinearity of the angular dispersion in leaky waveguides [Eq. (1)] suggests that a receiver with a fixed aperture will observe spectrum broadening and consequently temporal narrowing at smaller emission angles. Hence, we anticipate that the performance of temporal and spectral schemes would not be equivalent and would depend on the LOS and NLOS angles.

To test this hypothesis, we consider an experimental setting that consists of two paths, one LOS and one NLOS (with LOS and NLOS angles ranging from 25° to 75°), and explore the number of paths that can be detected according to either temporal or spectral characterization. In the temporal scheme, we distinguish paths based on their time of arrival. To this end, we apply a windowed FFT to the time-domain signals using a sliding Tukey window. At each step, we obtain the largest value of the spectrum and call it the Max-FFT value at that time delay.[17] The number of peaks in the (Max-FFT vs time delay) plot represents the number of paths. In contrast, in a spectral path detection scheme, we leverage the unique spectral content at each spatial angle and estimate the number of paths based on the peaks in the measured power spectrum. In Fig. 5, the inset shows the Max-FFT plot and the power spectrum plot for an example two-path configuration (LOS at 45° and NLOS at 30°). Both of these plots show two prominent peaks, one for each path. Figure 5 shows the accuracy percentage that the correct number of paths (two) is detected using these two different (but analogous) methods. This demonstration is consistent with the fact that the performance of temporal and spectral path detection schemes both depends on the LOS angle and that the observed trends can be anticipated from the physics of the emitter. Specifically, the temporal approach achieves better accuracy at smaller LOS angles as a narrow time-domain signal is less interfering (overlapping in time) with the weaker NLOS signal that arrives later. Similarly, the spectral approach performs better at larger LOS angles where the spectrum is narrow. This result also suggests a joint temporal–spectral scheme as a potential route toward a robust multipath detection approach.

Achievable Data Rate over NLOS Paths. Both SNR and bandwidth contribute to the capacity of a wireless channel or the achievable data rate. Reflected paths are typically expected to provide lower

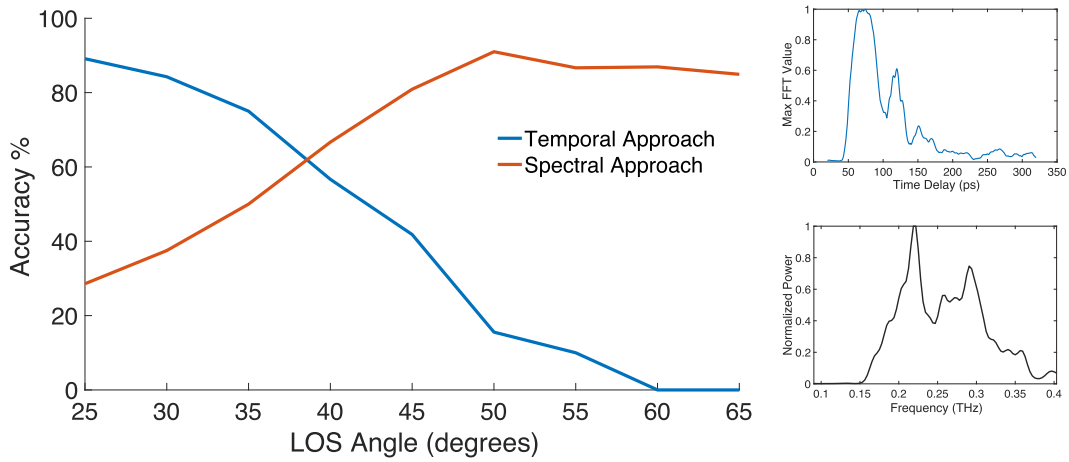

FIG. 5. The accuracy percentage of the temporal and spectral schemes for detecting the correct number of paths (two), when a LWA is employed at the TX. The temporal path characterization is more promising at smaller LOS angles while the spectral approach achieves better accuracy with larger LOS angles. The insets show the Max-FFT vs delay plot as well as the power spectrum for an example two-path setting (LOS at 45° and NLOS at 30°).

SNR due to extra propagation distance (compared to the LOS path) as well as additional dielectric and scattering losses as a result of interaction with reflecting surfaces. However, our results suggest that an NLOS path can actually support a higher data rate when a leaky-wave device is used as the transmitter. In contrast to a conventional transmitter, the supported bandwidth of a transmission from a leaky-wave antenna depends on the RX location and the wireless channel conditions. Particularly, the operating bandwidth for a receiver located in the far-field of the slot at an angle ϕ relative to the waveguide is given by the derivative of Eq. (1),[35]

$$BW(\phi) = \frac{df}{d\phi}\Delta\phi = \frac{c_0}{2b\,\sin\phi\,\tan\phi}\Delta\phi, \tag{2}$$

where $\Delta\phi$ is the effective angular aperture subtended by the receiver. Equation (2) indicates that the bandwidth is wider for lower emission angles. Hence, in a multipath setting, the supported bandwidth over a NLOS path with a smaller departure angle can be wider than a LOS path.

In Fig. 6, we illustrate this counter-intuitive result by plotting the disparity between operating bandwidth [Fig. 6(a)] and achievable data rate [Fig. 6(b)], comparing a LOS path configured at 45° against a NLOS path with varying angles of departure. First, in Fig. 6(a), we compare the measured half-power bandwidth at different NLOS angles relative to the measured bandwidth for a LOS path at 45°. It is clear from Fig. 6(a) that NLOS paths with departure angles smaller than 45° have wider bandwidth (up to >2.4× at 30°). We confirm these experimental observations with our model in

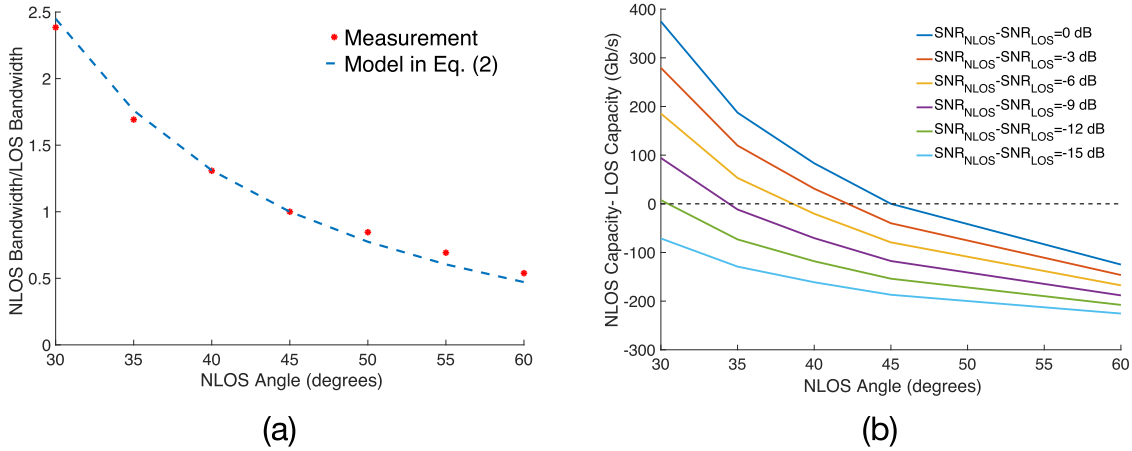

FIG. 6. Capacity analysis of LOS and NLOS paths: (a) Measured and theoretical BW at different NLOS departure angles relative to the supported BW of a LOS path at 45°. (b) The difference in the Shannon channel capacity between NLOS and LOS paths under different SNR conditions and different NLOS path angles relative to the leaky-wave transmitter antenna's axis for an assumed LOS path angle of 45°.

Eq. (2), indicating good agreement. Both SNR and bandwidth contribute to the capacity of a wireless channel or the achievable data rate, with the Shannon capacity given by $W \log_2(1 + SNR)$, where W denotes bandwidth. Next, we investigate the potential NLOS data rates relative to LOS data rate, given this disparity in bandwidth. In Fig. 6(b), the difference between the LOS and NLOS channel capacity is shown under different assumed SNR conditions and NLOS angles. When the channel losses are identical for the two paths (i.e., ignoring losses associated with the extra atmospheric propagation, free-space path loss, and the interaction with the reflector experienced by a signal propagating along the NLOS path), the channel capacity would be higher for NLOS departure angles below 45°. However, even if we assume an additional 9 dB of losses for the NLOS path, we predict that the channel capacity for certain NLOS angles is still larger than that of the LOS path due to the significant difference in supported bandwidth. We note that in indoor short-range (e.g., 1–10s of meters) use cases, the reflection loss is much larger than the additional free-space loss of the NLOS path (due to the increased traveled distance compared to the LOS). Furthermore, earlier work has shown that an additional loss of only 9 dB upon specular reflection from commonly encountered indoor surfaces is a reasonable expectation.[15] The disparity between LOS and NLOS bandwidths is directly linked to the geometric features of the RX and potential reflectors. Indeed, when the LOS angle is greater than that of NLOS, the situation is reversed, i.e., the LOS link can support wider bandwidth. This conclusion is a compelling illustration of the unique opportunities that distinguish THz wireless systems from those that operate at lower frequencies.

In conclusion, NLOS paths provide a rich and unique set of circumstances for THz networks. High-gain directional antennas can isolate a single path, thus reducing interference. Nonetheless, directionality also results in a higher sensitivity to RX alignment and creates new challenges in designing mobile THz wireless networks. Employing a leaky-wave antenna at the transmitter offers new opportunities for identifying different NLOS components of the channel and non-uniform bandwidth allocation that can yield higher data rates for reflected paths compared to the LOS configuration. This property of THz wireless links stems from using antennas that exhibit strong angular dispersion and differentiate it from conventional antennas, including those operating at lower frequencies.

This work was supported by the U.S. National Science Foundation and Army Research Lab (ARL).

DATA AVAILABILITY

The data that support the findings of this study are available from the corresponding author upon reasonable request.

REFERENCES

[1] I. E. Telatar and D. N. C. Tse, "Capacity and mutual information of wideband multipath fading channels," IEEE Trans. Inf. Theory **46**(4), 1384–1400 (2000).

[2] M. Patzold, *Mobile Fading Channels: Modelling, Analysis and Simulation* (John Wiley & Sons, Inc., 2001).

[3] Y. Ghasempour, M. K. Haider, C. Cordeiro, and E. W. Knightly, "Multi-user multi-stream mmWave WLANs with efficient path discovery and beam steering," IEEE J. Sel. Areas Commun. **37**(12), 2744–2758 (2019).

[4] H. P. Bui, Y. Ogawa, T. Nishimura, and T. Ohgane, "Performance evaluation of a multi-user MIMO system with prediction of time-varying indoor channels," IEEE Trans. Antennas Propag. **61**(1), 371–379 (2012).

[5] A. S. Y. Poon, R. W. Brodersen, and D. N. C. Tse, "Degrees of freedom in multiple-antenna channels: A signal space approach," IEEE Trans. Inf. Theory **51**(2), 523–536 (2005).

[6] L. Hanlen and M. Fu, "Wireless communication systems with-spatial diversity: A volumetric model," IEEE Trans. Wireless Commun. **5**(1), 133–142 (2006).

[7] A. Moldovan, M. A. Ruder, I. F. Akyildiz, and W. H. Gerstacker, "LOS and NLOS channel modeling for terahertz wireless communication with scattered rays," in *Proceedings of the IEEE GLOBECOM Workshops* (IEEE, 2014), pp. 388–392.

[8] M. Jacob, S. Priebe, A. Maltsev, A. Lomayev, V. Erceg, and T. Kürner, "A ray tracing based stochastic human blockage model for the IEEE 802.11ad 60 GHz channel model," in *Proceedings of the IEEE European Conference on Antennas and Propagation (EUCAP)* (IEEE, 2011), pp. 3084–3088.

[9] G. R. MacCartney, T. S. Rappaport, and S. Rangan, "Rapid fading due to human blockage in pedestrian crowds at 5G millimeter-wave frequencies," in *Proceedings of the IEEE Global Communications Conference (GLOBECOM)* (IEEE, 2017), pp. 1–7.

[10] V. Petrov, M. Komarov, D. Moltchanov, J. M. Jornet, and Y. Koucheryavy, "Interference and SINR in millimeter wave and terahertz communication systems with blocking and directional antennas," IEEE Trans. Wireless Commun. **16**(3), 1791–1808 (2017).

[11] S. Abadal, C. Han, and J. M. Jornet, "Wave propagation and channel modeling in chip-scale wireless communications: A survey from millimeter-wave to terahertz and optics," IEEE Access **8**, 278–293 (2020).

[12] C. Jansen, R. Piesiewicz, D. Mittleman, T. Kürner, and M. Koch, "The impact of reflections from stratified building materials on the wave propagation in future indoor terahertz communication systems," IEEE Trans. Antennas Propag. **56**(5), 1413–1419 (2008).

[13] R. Piesiewicz, M. Jacob, M. Koch, J. Schoebel, and T. Kürner, "Performance analysis of future multigigabit wireless communication systems at THz frequencies with highly directive antennas in realistic indoor environments," IEEE J. Sel. Top. Quantum Electron. **14**(2), 421–430 (2008).

[14] S. Priebe and T. Kürner, "Stochastic modeling of THz indoor radio channels," IEEE Trans. Wireless Commun. **12**(9), 4445–4455 (2013).

[15] J. Ma, R. Shrestha, L. Moeller, and D. M. Mittleman, "Channel performance of indoor and outdoor terahertz wireless links," APL Photonics **3**, 051601 (2018).

[16] J. Ma, R. Shrestha, W. Zhang, L. Moeller, and D. M. Mittleman, "Terahertz wireless links using diffuse scattering from rough surfaces," IEEE Trans. Terahertz Sci. Technol. **9**, 463–470 (2019).

[17] Y. Amarasinghe, R. Mendis, and D. M. Mittleman, "Real-time object tracking using a leaky THz waveguide," Opt. Express **28**, 17997–18005 (2020).

[18] S. Jia, L. Zhang, S. Wang, W. Li, M. Qiao, Z. Lu, N. M. Idrees, X. Pang, H. Hu, X. Zhang, L. K. Oxenløwe, and X. Yu, "2 × 300 Gbit/s line rate PS-64QAM-OFDM THz photonic-wireless transmission," J. Lightwave Technol. **38**(17), 4715–4721 (2020).

[19] S. Jia, X. Yu, H. Hu, J. Yu, P. Guan, F. Da Ros, M. Galili, T. Morioka, and L. K. Oxenløwe, "THz photonic wireless links with 16-QAM modulation in the 375-450 GHz band," Opt. Express **24**(21), 23777–23783 (2016).

[20] A. Hirata, T. Kosugi, H. Takahashi, J. Takeuchi, H. Togo, M. Yaita, N. Kukutsu, K. Aihara, K. Murata, Y. Sato, T. Nagatsuma, and Y. Kado, "120-GHz-band wireless link technologies for outdoor 10-Gbit/s data transmission," IEEE Trans. Microwave Theory Tech. **60**(3), 881–895 (2012).

[21] N. Krumbholz, K. Gerlach, F. Rutz, M. Koch, R. Piesiewicz, T. Kürner, and D. Mittleman, "Omnidirectional terahertz mirrors: A key element for future terahertz communication systems," Appl. Phys. Lett. **88**, 202905 (2006).

[22] S. Ju, S. H. Ali Shah, M. A. Javed, J. Li, G. Palteru, J. Robin, Y. Xing, O. Kanhere, and T. S. Rappaport, "Scattering mechanisms and modeling for terahertz wireless communications," in *IEEE International Conference on Communications (ICC)* (IEEE, 2019), pp. 1–7.

[23] C. Jansen, S. Wietzke, D. Mittleman, M. Koch, and T. Kürner, "Properties of building and plastic materials in the THz range," Int. J. Infrared Millimeter Waves **28**, 363–371 (2007).

[24]R. Piesiewicz, C. Jansen, D. Mittleman, T. Kleine-Ostmann, M. Koch, and T. Kürner, "Scattering analysis for the modeling of THz communication systems," IEEE Trans. Antennas Propag. **55**(11), 3002–3009 (2007).
[25]C. Jansen, S. Priebe, C. Moller, M. Jacob, H. Dierke, M. Koch, and T. Kürner, "Diffuse scattering from rough surfaces in THz communication channels," IEEE Trans. Terahertz Sci. Technol. **1**(2), 462–472 (2011).
[26]S. Priebe, M. Jacob, C. Jansen, and T. Kürner, "Non-specular scattering modeling for THz propagation simulations," in *Proceedings of the IEEE European Conference on Antennas and Propagation (EUCAP)* (IEEE, 2011), pp. 1–5.
[27]K. Guan, B. Peng, D. He, J. M. Eckhardt, S. Rey, B. Ai, Z. Zhong, and T. Kürner, "Channel characterization for intra-wagon communication at 60 and 300 GHz bands," IEEE Trans. Veh. Technol. **68**(6), 5193–5207 (2019).
[28]M. van Exter and D. R. Grischkowsky, "Characterization of an optoelectronic terahertz beam system," IEEE Trans. Microwave Theory Technol. **38**, 1684–1691 (1990).
[29]P. U. Jepsen and S. R. Keiding, "Radiation patterns from lens-coupled terahertz antennas," Opt. Lett. **20**(8), 807–809 (1995).
[30]J. Van Rudd and D. M. Mittleman, "Influence of substrate-lens design in terahertz time-domain spectroscopy," J. Opt. Soc. Am. B **19**(2), 319–329 (2002).
[31]J. Ma, N. J. Karl, S. Bretin, G. Ducournau, and D. M. Mittleman, "Frequency-division multiplexer and demultiplexer for terahertz wireless links," Nat. Commun. **8**, 729 (2017).
[32]Y. Ghasempour, R. Shrestha, A. Charous, E. Knightly, and D. M. Mittleman, "Single-shot link discovery for terahertz wireless networks," Nat. Commun. **11**, 2017 (2020).
[33]Y. Ghasempour, C.-Y. Yeh, R. Shrestha, D. M. Mittleman, and E. Knightly, "Single shot single antenna path discovery in THz networks," in *Proceedings of the 26th Annual International Conference on Mobile Computing and Networking (MobiCom), London, September 2020* (ACM, 2020), No. 18, pp. 1–13.
[34]S. Gupta, S. Abielmona, and C. Caloz, "Microwave analog real-time spectrum analyzer (RTSA) based on the spectral-spatial decomposition property of leaky-wave structures," IEEE Trans. Microwave Theory Tech. **57**(12), 2989–2999 (2009).
[35]Y. Ghasempour, C. Yeh, R. Shrestha, Y. Amarasinghe, D. M. Mittleman, and E. Knightly, "LeakyTrack: Non-coherent single-antenna nodal and environmental mobility tracking with a leaky-wave antenna," in Proceedings of the 18th ACM Conference on Embedded Networked Sensor Systems (ACM, 2020), pp. 56–68.
[36]N. J. Karl, R. W. McKinney, Y. Monnai, R. Mendis, and D. M. Mittleman, "Frequency division multiplexing in the terahertz range using a leaky wave antenna," Nat. Photonics **9**, 717–720 (2015).